

# **AUTOMATIC COMPENSATION OF PRESSURE EFFECTS ON SMART FLOW SENSORS IN THE ANALOG AND DIGITAL DOMAIN**

M. Piotto<sup>a</sup>, A.N. Longhitano<sup>b</sup>, F. Del Cesta<sup>b</sup>, P. Bruschi<sup>b</sup>

<sup>a</sup>IEIIT-Pisa, CNR, via G. Caruso 16, I-56122, Pisa, Italy

<sup>b</sup>Dipartimento di Ingegneria dell'Informazione, University of Pisa, via G. Caruso 16, I-56122 Pisa,

Italy

## **Abstract**

Two different approaches for the automatic compensation of pressure effects on thermal flow sensors are investigated. One approach operates in the analog domain and it is based on a closed-loop circuit that uses a pressure dependent signal to keep the sensor output constant. The digital approach operates in an open loop fashion and is capable of producing also a pressure reading. The effectiveness of the proposed methods has been verified by means of a smart flow sensor integrating on the same chip the sensing structures and a configurable electronic interface performing signal reading and non idealities compensation. The chip has been designed with a commercial CMOS process and fabricated by means of a post-processing technique. The experimental results performed in nitrogen confirm that both methods are capable of reducing the sensitivity of the flow sensor output signal to pressure variations.

**Keywords:** Smart sensor; thermal flow sensor; pressure compensation; micro-electro-mechanical systems (MEMS)

Corresponding Author:

Massimo Piotto,

IEIIT-Pisa, CNR,

via G. Caruso 16,

I-56122, Pisa, Italy

Tel +39 050 2217657,

Fax +39 050 2217522,

e-mail: massimo.piotto@ieiit.cnr.it

## 1. Introduction

Measurement of gas flow rate is an essential requirement in many application fields including automotive and process industry, indoor climate control and biomedical instrumentation. Different solutions have been proposed and many commercial products are available in the market. The advent of the MEMS (Micro-Electro-Mechanical Systems) technology in the late 1980s paved the way to the design and fabrication of novel micrometric devices characterized by low power consumption, fast response times and reduced weights [1-4]. Micromachined flow sensors based on a thermal principle are without doubts the most investigated devices and a few commercial products are now available. One of the reasons of their success is that the sensor structure is quite simple and can be fabricated adding a few steps to a standard microelectronic process. This allows integrating on the same chip both the sensors and the read-out electronics with advantages in terms of immunity to electromagnetic interferences [5-7]. The increasing sophistication of micromachining technology has stimulated the integration of different sensors on the same chip in order to extract simultaneously different flow parameters, a requirement that is essential to attain accurate measurements. The integration of flow and pressure sensors on the same silicon chip was demonstrated by [8]; nevertheless this result was obtained by combining different technologies, with the drawback of added costs and fabrication complexity. Multi-parameter measurements based on a single sensing structure have also been proposed [9, 10].

The dimensions of the sensing structures in the micrometer range introduce also some drawbacks including sensitivity to gas rarefied effects even near the atmospheric pressure [11]. This property has been advantageously exploited to fabricate miniaturized Pirani-type vacuum sensors with measurement range around atmospheric pressure [12]. Nevertheless, pressure sensitivity causes inaccuracy in applications where the flow sensor has to operate in sub-atmospheric ranges like in the gas lines of

semiconductor process chambers [13]. Typical compensation schemes use an additional sensor to read the pressure and calculate the correction to be applied to the flow rate sensor output.

Recently we have developed a novel method to obtain information of the gas pressure from the same sensing structure used for flow detection [14]. The method has been developed for thermal flow sensors based on the well known differential micro-calorimeter principle. These sensors typically consist of a heater symmetrically placed between two temperature sensors. While the flow-sensitive signal is proportional to the temperature difference between the two temperature sensors (differential signal), a second signal, proportional to the mean of the overheating of the two temperature sensors (common mode signal), can be extracted from the sensor. We observed that the common mode signal can be used to detect the gas pressure for compensation purposes. An all-analog approach based on this principle has been developed and validated by means of a purposely built circuit, implemented with discrete components on printed circuit board (PCB). Recently, we have developed a single chip solution, consisting in a smart flow sensor with a low-noise-on-chip electronic interface implementing the proposed pressure compensation [15]. This smart **sensor** uses dual heater sensing structure to obtain also cancellation of the sensor offset and offset drift with the approach **described** in [16].

In this work, we describe the result of experimental tests performed on this single-chip smart sensor in nitrogen flow, demonstrating the effectiveness of the pressure compensation capability of the interface. We also propose an alternative solution, consisting in processing the two signals (differential and common mode) produced by the sensor using a numerical algorithm. Experimental results shown in this paper demonstrate that, with this “digital” approach, it is possible to produce accurate measurements of both the gas pressure and flow rate from a single sensing structure.

## 2. Device description and fabrication

The chip has been designed with the BCD6s process of STMicroelectronics and a post-processing technique has been applied to thermally insulate the sensing structures from the substrate. In Fig. 1 an optical micrograph of the chip area including the sensors and the electronic interface is shown. Details about the chip design and fabrication have been reported in [15]. A brief description of the sensors, the electronic interface and the device packaging is reported in the following sections.

### 2.1 Sensors

The sensors consist of two heaters placed between an upstream and a downstream temperature probe. The heaters are polysilicon **resistors** placed over suspended dielectric membranes while the temperature probes are **thermopiles** formed by 10  $n^+$ poly/ $p^+$ poly thermocouples. The hot contact of the thermocouples is placed at the tip of a cantilever beam while the cold contact is over the silicon substrate. An optical microscope micrograph of a sensing structure is shown in Figure 2 (a).

The detection principle is similar to that of conventional calorimetric flow sensors: the thermopiles individually measure the downstream and upstream overheating of the cantilever tips, produced by the heat flux from the heaters; the gas flow produces an asymmetry in the temperature distribution, which is sensed by the thermopiles. The output voltage of the sensor is the difference between the voltages  $V_{T1}$  and  $V_{T2}$  produced by the two thermopiles and proportional to the upstream and downstream overheating, respectively. The adoption of double heater architectures allows intrinsic offset compensation by means of the power unbalance of the two heaters [16].

The post-processing procedure used to fabricate the sensors consists in two main steps: (i) the selective removal of the passivation and inter-metallic dielectric layers to access the bare silicon from the chip front-side and (ii) the silicon anisotropic etching. The dielectric layers have been selectively removed by means of a photolithographic step followed by a silicon dioxide reactive ion etching (RIE) in

CF<sub>4</sub> / Ar (50% / 50%) gas mixture. The silicon substrate has been anisotropically etched in a solution of 100 g of 5 wt% TMAH with 2.5 g of silicic acid and 0.7 g of ammonium persulfate. Due to the selectivity of this solution towards silicon dioxide and aluminum, no additional masks has been used to protect integrated microelectronic circuits and pads during the etching.

The SEM (scanning electron microscope) micrograph in Fig. 2 (b) has been acquired after the silicon etching at 85 °C for 105 minutes. The visible cavity in the silicon guarantees the thermal insulation of both the heaters and the hot contacts of the thermocouples from the substrate. Thermopile and heater morphology is not visible since they are buried under a thick SiO<sub>2</sub> dielectric layer.

## 2.2 *Electronic interface*

The on-chip interface is a versatile system that is capable of performing several operations. A simplified block diagram is shown in Figure 3, where also connections to a sensing structure is represented. A programmable heater driver produces the two currents  $I_{H1}$  and  $I_{H2}$  required to bias the sensor heaters. The mean value of the two currents is proportional to the output voltage of the error amplifier, while the current ratio  $I_{H1}/I_{H2}$  is programmable through an 8 bit digital word (offset null). Current ratios different from 1 introduce a power unbalance between the heaters that, once properly calibrated, cancels the sensor offset. This approach presents the advantage to strongly reduce also the offset drift [16] originating from the temperature dependence of the gas thermal conductivity.

The differential voltage produced by the sensor is amplified by an ultra low noise fully-differential amplifier ( $A_D$ ). Chopper modulation is used to obtain an input noise voltage density low enough to be negligible with respect to the sensor thermal noise. In this way the sensor intrinsic resolution is not altered by the amplifier. The measured residual input offset is less than 1  $\mu$ V. The individual thermopile voltages,  $V_{T1}$  and  $V_{T2}$ , proportional to the thermopile hot junction overheating, are also separately amplified ( $A_1$ ), and the resulting signals are made available as additional output signals for possible further off-chip processing. These two signals are also fed to an internal block (CM extractor)

that produces a signal proportional to the common mode voltage ( $V_C$ ) of the thermopile outputs. This signal is compared to a reference signal  $V_{CREF}$  by the differential amplifier ( $A_2$ ) producing a pressure sensitive signal used to drive the sensor heaters in a closed loop fashion. This loop embodies the analog pressure compensation approach described in next section.

The pressure compensation function can be disabled by changing the status of switch  $S_M$ . In this way the constant voltage  $V_{DRV}$  (programmable in four levels) is used to stimulate the heater driver (V-I converter and current splitter). This configuration, corresponding to traditional open loop, constant current operating mode, is used to implement the digital approach described later. A standard three-wire serial interface is used to program an internal register that sets the gain of the various amplifiers, changes the current ratio (offset null) and determines the status of  $S_M$ . A detailed description of the topology of the main blocks composing the on-chip interface is present in Ref.[15].

### *2.3 Package*

In order to connect the device to a gas line and convey the flow to the integrated sensing structure, a poly-methyl-methacrylate (PMMA) package was purposely designed and fabricated. The package is the result of the development the low-cost packaging method, firstly proposed in [17], which is based on a PMMA block that can feed multiple gas flows to different areas of a chip [18]. As schematically shown in Fig. 4, the package consists of three different parts: a conveyor, an adapter and a pipe connector.

The conveyor has an optically front flat face slightly smaller than the chip pad frame. Three trenches, communicating with the opposite section of the conveyor through holes of 0.6 mm diameter, are milled on the conveyor flat face by means of a precision computer controlled milling machine (VHF CAM 100). In Fig. 4 a conveyor with only two trenches (not visible) and four holes is shown for simplicity. The conveyor is applied to the chip front surface by means of a guide, previously aligned by means of a micrometric displacement stage. A thin cyanoacrylate layer is manually deposited on the adapter front

surface prior to applying to the chip. Gentle pressure between the two parts causes the glue to spread on the contact surface, sealing the trenches. The structure is reinforced by filling the chip chamber with cyanoacrylate glue that fixes the conveyor to the ceramic package.

After conveyor gluing, the alignment guide was removed. In order to connect the device to 1.2 mm diameter pipes of a reference gas line, a PMMA adapter was designed. The purpose of the adapter is to increase the distance between the holes of the conveyor by means of trenches, allowing the connection of greater pipes. A PMMA connector was finally designed to seal the adapter trenches and connect the device to stainless steel pipes. The adapter and the connector were aligned to the conveyor using an optical microscope and they were glued each other with cyanoacrylate glue. In Fig. 5 a photo of the assembled device is shown.

### 3. Principle of operation

In order to understand the proposed methods, it is important to consider how the two signals produced by the sensor, namely the differential voltage  $V_D$  and the common mode voltage  $V_C$ , depend on pressure ( $P$ ) and flow rate ( $Q$ ). Fig. 6 (a) shows the dependence on flow rate of both voltages at constant pressure. The important fact is that, while  $V_D$  is strongly flow sensitive (hence the flow detection principle), the mean value  $V_C$  is practically flow independent. On the other hand, Fig. 6 (b) shows that  $V_D$  and  $V_C$  exhibit similar dependence on pressure. This suggested to use voltage  $V_C$  as a pressure detector, since its cross sensitivity to flow rate can be neglected in a first order approximation at least in the range of relatively small flow rates. The information on pressure gained in this way, is used to compensate the pressure dependence of the differential signal  $V_D$ . The particular dependence of  $V_D$  and  $V_C$  on pressure lends itself to an elegant analog approach [14], completely implemented by the on-chip electronic interface depicted in Fig. 3. The digital approach, currently implemented with external subsystems, pushes this concept forward, allowing simultaneous detection of pressure and flow rate with a single sensor. The two approaches are described in the following subsections.

### 3.1 Analog approach

With the analog approach, the variations of signal  $V_C$  caused by pressure are used to apply a proper change in the heater current. This method is based on a simple empirical model proposed in [14] that approximates the dependence of signals  $V_D$  and  $V_C$  on pressure ( $P$ ), flow rate( $Q$ ) and heater power ( $W$ ) with the following equations:

$$\begin{aligned} V_D &= W \cdot f_D(Q, P) \\ V_C &= W \cdot f_C(Q, P) \end{aligned} \quad (1)$$

Neglecting the dependence of the common mode signal  $V_C$  on flow rate, the functions  $f_{D,C}$  can be written as:

$$\begin{aligned} f_D(Q, P) &= f_D(Q, \infty) \frac{P}{P + P_{trD}} \\ f_C(P) &= f_C(\infty) \frac{P}{P + P_{trC}} \end{aligned} \quad (2)$$

where,  $f_D(Q, \infty)$  and  $f_C(\infty)$  describes the asymptotic behavior of  $V_D$  and  $V_C$  at high pressures and  $P_{trD}$  and  $P_{trC}$  are the transition pressures of  $V_D$  and  $V_C$ , respectively. According to equation (1), it is possible to use the heater power  $W$  to compensate the variations of  $V_D$  and  $V_C$  due to pressure.

The analog approach is based on an electronic circuit capable of operating as a closed-loop controller that tends to keep the signal  $V_C$  constant. Unfortunately, the relative sensitivity to pressure of  $V_D$  and  $V_C$  are different, as confirmed by the experimental data reported in Fig 6 (b) where a separation between the two curves is clearly visible. In particular, the effects of pressure on signal  $V_C$  begin to be relevant at higher pressures, i.e. the  $P_{trC}$  turned out to be significantly greater than  $P_{trD}$  ( $P_{trC} = 12$  hPa,  $P_{trD} = 6$  hPa). This means that keeping the signal  $V_C$  strictly constant (with an high loop gain) would result in overcompensating the differential voltage  $V_D$ , that, ultimately, is the signal of interest. For this reason the value of the loop gain should be precisely set in order to obtain an optimum compensation. We demonstrated [14] that the optimum value of the loop gain is given by:



$$A_{LOPT} = \left( \frac{P_{trC}}{P_{trD}} - 1 \right)^{-1} \quad (3)$$

The optimum gain loop can be calculated from the knowledge of physical parameters of the sensors, and in particular from the transition pressures of the differential and common mode voltages, that can be measured with a single pressure scan.

The analog approach is implemented with the integrated circuit of Fig. 3 operating in the closed loop mode setting switch  $S_M$  on position 1. The pressure compensation subsystem operates in a negative feedback fashion so that a pressure decrease causes a heater current increase compensating the pressure-induced drop of signals  $V_D$  and  $V_C$ . The subsystem is implemented by means of switched capacitor circuits, operating at the same frequency as the chopper amplifier  $A_D$  but with a quadrature clock, in order to minimize intermodulation effects that would result in degraded offset performances. Correlated double sampling is used to minimize the impact of offset and low frequency noise in this part of the interface. Fine tuning of the loop gain is obtained by digitally programmable gains ( $A_1$ ,  $A_2$ ). Note that the heater current increase, necessary for the pressure compensation operation, is operated while maintaining the optimum current ratio for offset compensation.

### 3.2 Digital approach

This method requires that voltages  $V_D$  and  $V_C$  are acquired operating the heaters at constant current by setting switch  $S_M$  on position 2. As in the analog approach described above, proper current unbalance is applied by the current splitter in order to obtain an optimal offset cancellation. A microcontroller board, equipped with high precision, multichannel Analog-to-Digital Converters (ADC) is used to acquire the chip output voltages  $A_D V_D$  and  $A_1 V_{T1}$  and  $A_2 V_{T2}$ . These data are transmitted to a Personal Computer where a program written in an high level language (Python with scientific packages “numpy” and “scipy”) estimates the voltages  $V_D$  and  $V_C$  taking into account also the non linearity of the on-chip amplifier responses, previously measured. The actual dependence of  $V_D$  and  $V_C$  on pressure and flow

rate, generically represented by equation (1), is experimentally characterized by means of a series of measurements, performed on a dense mesh of  $Q, P$  points distributed in the  $Q, P$  domain of interest. The fact that  $f_C$ , differently from  $f_D$ , exhibit a very weak dependence on  $Q$ , guarantees that  $f_D$  and  $f_C$  are independent functions. Furthermore, both  $f_D$  and  $f_C$  monotonically increase with pressure, while the dependence of  $f_D$  on  $Q$  is also monotonic over relatively large flow rate ranges. These properties permit the inversion of the equation set (1) in order to estimate  $Q$  and  $P$  from the signals  $V_D$  and  $V_C$ . Inversion is numerically performed in the digital domain by means of a proper algorithm implemented on the personal computer that processes the measured  $V_D, V_C$  in real time and yield the estimated pressure and flow rate values.

#### **4. Experimental results**

Measurements have been performed by connecting the sample to a reference nitrogen line equipped with a 10 sccm flow controller (MKS 1179B), an absolute pressure gauge (MKS 750B) and a rotary vacuum pump connected to the exhaust end of the line through a pin valve, as schematically shown in Fig.7. The device under test was placed between the pressure gauge and the pin valve. A purposely built printed circuit board equipped with an ADuC847 (Analog Devices) microcontroller and communicating with a personal computer was used to program the chip registers and to read the analog voltages.

The measurement procedure was the following. At the beginning the flow rate was set to zero and the pin valve was completely opened to allow the line vacuum. Then the flow rate was fixed by the controller and the pin valve was gradually closed; the resulting pressure was read with the pressure gauge.

#### 4.1 Experimental results obtained with the analog approach

Figure 8 shows the output voltage in zero flow condition (offset voltage) as a function of pressure. Note that the non calibrated offset exhibits a large dependence on pressure. The offset correction procedure is effective in eliminating this additional source of pressure sensitivity that would affect conventional single heater sensors.

The dependence of the output voltage on pressure has been measured for three different flow rate values and the results are shown in Fig. 9. In order to emphasize the advantages of the proposed device, the curves obtained with the same sample without the pressure compensation circuit (open loop) are reported in the same figure. The curves measured using the closed-loop configuration show a less than 2% residual pressure dependence in the explored pressure range.

These results confirm that pressure insensitive flow rate measurements can be effectively obtained with the proposed single chip sensor.

#### 4.2 Experimental results obtained with the digital approach

In the preliminary phase (sensor calibration), a series of measurements for 100 different pressure/flow rate pairs have been performed in nitrogen **in order** to build the mesh of experimental data. The pressure was varied between 40 hPa and 1024 hPa and the flow rate from 0 to 15 sccm. In order to improve the inversion algorithm, the mesh was artificially thickened using spline interpolation formulas for both the  $P$  and  $Q$  dependence. The contour plots in Fig.10 illustrate the dependence of  $V_D$  and  $V_C$  on pressure and flow rate, as resulting from measurements performed on a sample with the heaters fed with a 0.75 mA current (nearly 1 mW per heater). The shape of the  $V_D$  and  $V_C$  contour curves visually suggests that, in the explored range, there is only an intersection point (i.e. a  $P, Q$  pair) for each  $V_D, V_C$  pair, confirming the possibility of univocally determining both pressure and flow rate from simultaneous measurement of  $V_D$  and  $V_C$ .

The second phase of the digital approach validation was aimed to simulate the use of the sensor in operating conditions. The pressure and flow rate were varied over the same interval used for the initial calibration and the pressure/flow rate estimates produced by the algorithm were compared with the reference instrument readings. An example of the sensor response to pressure variations from 40 to 360 hPa performed at a constant flow rate of 7.2 sccm is shown in Fig.11. Note that all the pressure and flow rate values in this experiment were different from the points used to build the mesh. A good accuracy in terms of both pressure and flow rate measurement can be observed.

## 5. Conclusions

The experiments shown in this paper were aimed to evaluate the performance of a recently developed single-chip smart flow sensor, whose architecture was presented in Ref. [15]. Tests performed in nitrogen at various pressures and flow rates indicated that the analog loop is very effective in reducing the sensitivity to pressure. This result was facilitated also by the particular technique adopted to cancel the sensor offset, that otherwise would introduce additional pressure dependent terms. The proven low pressure sensitivity and extreme compactness of this smart sensor make it suitable for incorporation in miniaturized mass flow control for the distribution of low pressure gas flows. Extension to different gas types, marked by different transition pressures, can be simply obtained by tuning the on-chip amplifier gains through the internal registries.

Limitations of the approach at very low pressure is given by the maximum power that can be withstood by the heaters, since the analog loop compensate the sensitivity decrease by boosting the heater current.

A digital, open loop approach that overcomes this limitation and, at the same time, is capable of producing also a pressure reading has been proposed and experimentally validated. At present, the

digital approach requires an external computational unit but future single-chip implementations that exploit the availability of low cost compact digital processing cores can be reasonably envisioned.

## **Acknowledgements**

The authors would like to thank the R & D group of the STMicroelectronics of Cornaredo (MI, Italy) for fabrication of the chips described in this work.

## **References**

- [1] B.W. van Oudheusden, Silicon thermal flow sensors, *Sens. Actuators A: Phys.* 30 (1992) 5–26.
- [2] N. T. Nguyen, Micromachined flow sensors – A review, *Flow Meas. Instrum.* 8 (1997) 7–16.
- [3] Y.-H. Wang, C.-P. Chen, C.-M. Chang, C.-P. Lin, C.-H. Lin, L.-M. Fu, C.-Y. Lee, MEMS-based gas flow sensors, *Microfluid. Nanofluid.* 6 (2009) 333–346.
- [4] J. T. W. Kuo, L. Yu, E. Meng, Micromachined Thermal Flow Sensors—A Review, *Micromachines* 3 (2012) 550-573.
- [5] E. Yoon, K. D. Wise, An integrated mass flow sensor with on-chip CMOS interface circuitry, *IEEE Trans. Electron Dev.* 39 (1992) 1376–1386.
- [6] F. Mayer, A. Haberli, H. Jacobs, G. Ofner, O. Paul, H. Baltes, Single-chip CMOS anemometer, in *Proc. Int. Electron Dev. Meet.*, Washington, DC, Dec. 7-10, 1997, pp. 895–898.
- [7] K. A. A. Makinwa, J. H. Huijsing, A wind-sensor with integrated interface electronics, in *Proc. IEEE Int. Symp. Circuits Syst.*, Sydney May 6-9, 2001, pp. 356–359.
- [8] E. Kälvesten, C. Vieider, L. Löfdahl, G. Stemme, An integrated pressure-flow sensor for correlation measurements in turbulent gas flows, *Sensors and Actuators A* 52, (1996) 51-58.
- [9] J. van Kuijk, T.S.J. Lammerink, H.-E. de Bree, M. Elwenspoek, J.H.J. Fluitman, Multi-parameter detection in fluid flows, *Sensors and Actuators A* 47, (1995) 369-372.

- [10] D. F. Reyes Romero, K. Kogana, A. S. Cubukcu, , G. A. Urban, Simultaneous Flow and Thermal Conductivity Measurement of Gases Utilizing a Calorimetric Flow Sensor, *Sensors and Actuators A*, in press.
- [11] P. Bruschi, M. Piotta, G. Barillaro, Effects of gas type on the sensitivity and transition pressure of integrated thermal flow sensors, *Sens. Actuators A* 131 (2006) 182–187.
- [12] R. Puers, S. Reyntjens, D. De Bruyker, The NanoPirani – An extremely miniaturized pressure sensor fabricated by focused ion beam rapid prototyping, *Sens. Actuators A* 97–98 (2002) 208–214.
- [13] N. Urdaneta, J. Krell, B. Brown, Thermal-based mass flowcontrol for SDS gas delivery systems, *Solid State Technol.* 42 (1999) 59–65.
- [14] P. Bruschi, M. Dei, M. Piotta, A method to compensate the pressure sensitivity of integrated thermal flow sensors, *IEEE Sensors J.* 10 (2010) 1589–1597.
- [15] M. Piotta, M. Dei, F. Butti, G. Pennelli, P. Bruschi, Smart flow sensor with on-chip CMOS interface performing offset and pressure effect compensation, *IEEE Sensors J.* 12 (2012) 3309-3317.
- [16] P. Bruschi, M. Dei, M. Piotta, An offset compensation method with low residual drift for integrated thermal flow sensors, *IEEE Sensors J.* 11 (2011) 1162–1168.
- [17] P. Bruschi, V. Nurra, M. Piotta, A compact package for integrated silicon thermal gas flow meters, *Microsyst. Technol.* 14, (2008) 943–949.
- [18] P. Bruschi, M. Dei, M. Piotta, A single chip, double channel thermal flow meter, *Microsyst. Technol.* 15 (2009) 1179–1186.

## **Authors Biographies**

*Massimo Piotto:* Massimo Piotto was born in 1970, La Spezia, Italy. He received his laurea degree in Electronic Engineering from the University of Pisa, Italy, in 1996 and his Ph.D. degree in Electronic, Computer and Telecommunication Engineering in 2000. Since December 2001 he has been a researcher of the section of Pisa of the “Istituto di Elettronica e di Ingegneria dell’Informazione e delle Telecomunicazioni” - National Research Council. His main research interests concern micromachining, MEMS, microelectronic and nanoelectronic devices and technologies.

*Aurelio Nunzio Longhitano:* Aurelio Nunzio Longhitano was born in Bronte, Italy, and received the M.Sc. in Electronic Engineering from The University of Pisa, Italy, in 2011. Since January 2012 he is Ph.D. student in Information Engineering at the Information Engineering Department of The University of Pisa. Analog Electronics and Sensor Interfaces are his main areas of interest.

*Francesco Del Cesta:* Francesco Del Cesta was born in 1986 in Pisa, Italy. He received his Laurea degree in Electronic Engineering from the University of Pisa in July 2012. Francesco Del Cesta is currently a Ph.D. student at the Department of Information Engineering of the University of Pisa. His main area of interest is the design of analog and mixed-signal integrated circuits for sensor interfacing.

*Paolo Bruschi:* Paolo Bruschi was born in Massa, Italy, in 1964. He received the laurea degree in Electronic Engineering from the University of Pisa, Italy, in 1989. In 1993 he joined the Department of Information Engineering as a researcher. He is currently an associate professor of the Department of Information Engineering of the University of Pisa. His main area of interest is the development of integrated silicon sensors and actuators. He is also involved in the design of analog integrated circuits and the development of process simulators.

## Figure Captions.

Figure 1: Photo of the chip area including the electronic interface and the sensing structures after the post-processing.

Figure 2: Optical microscope (a) and SEM (b) image of a double heater structure after the silicon removal in a TMAH solution (H1, H2: heaters over suspended SiO<sub>2</sub> membranes; TC1, TC2: thermopiles).

Figure 3: Block diagram illustrating the sensor, the differential voltage ( $V_{T2}-V_{T1}$ ) amplifier and the subsystem for the pressure compensation based on the negative feedback.

Figure 4: Exploded view of the packaging.

Figure 5: Photograph of the assembled device

Figure 6: Differential and common mode voltages as a function of flow rate (a) and pressure (b). Experiments are performed in Nitrogen.

Figure 7: Measurement set-up used for sensor characterization: DUT indicates the device under test and MFC a mass flow controller.

Figure 8: Output offset voltage (zero flow) dependence on pressure measured with the same current applied to the heaters (not calibrated) and the proper current unbalance (calibrated) for offset compensation.

Figure 9: Output voltage dependence on pressure at three different flow rates measured with open-loop and closed-loop heater driving method.

Figure 10: Contour plots representing the (interpolated) dependence of  $V_D$  and  $V_C$  on pressure and flow rate. The pressure range has been slightly extended beyond the experimental range using the fitting functions.

Figure 11: Example of flow rate and pressure data estimation performed at various pressure values and 7.2 sccm fixed flow rate (Nitrogen).



# FIGURES

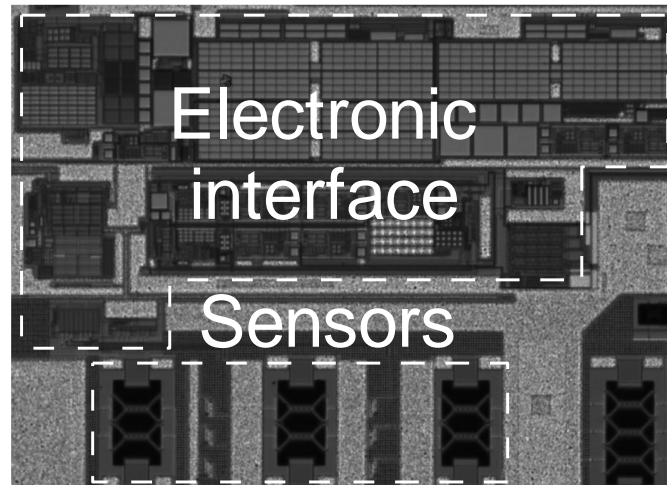


Figure 1

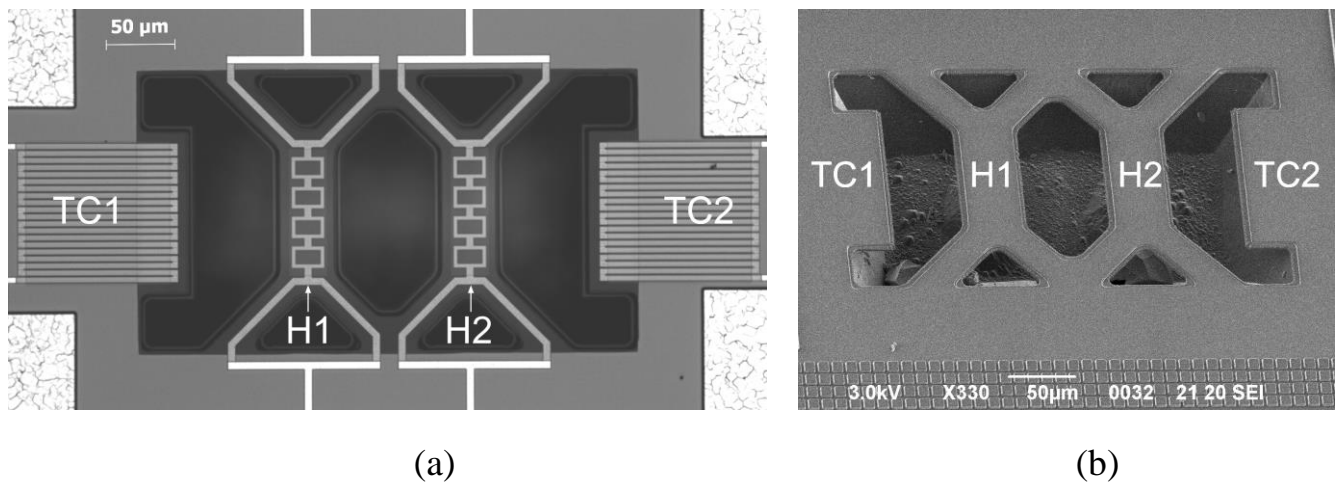


Figure 2

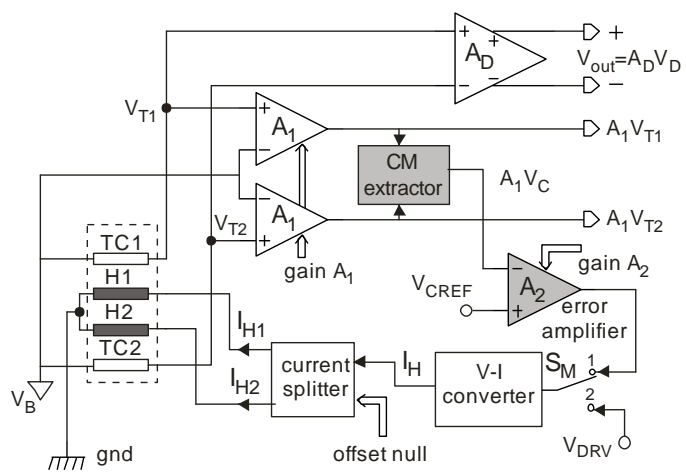


Figure 3

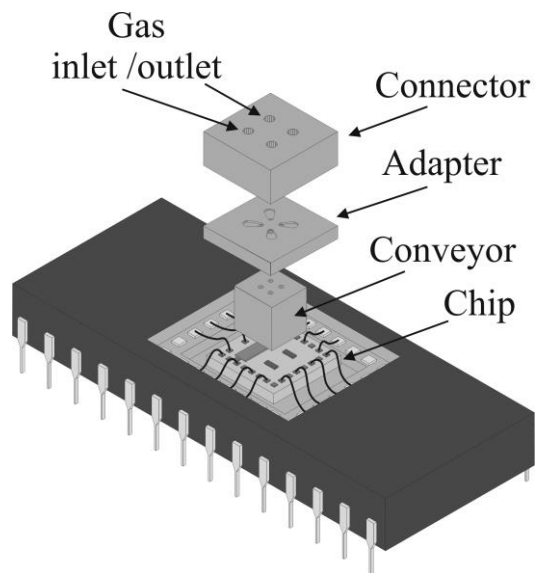


Figure 4

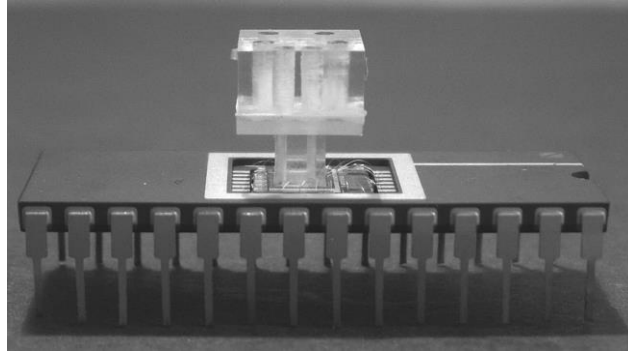


Figure 5

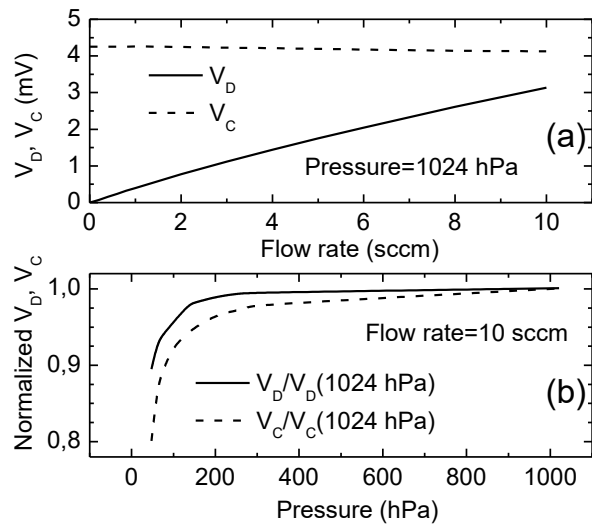


Figure 6

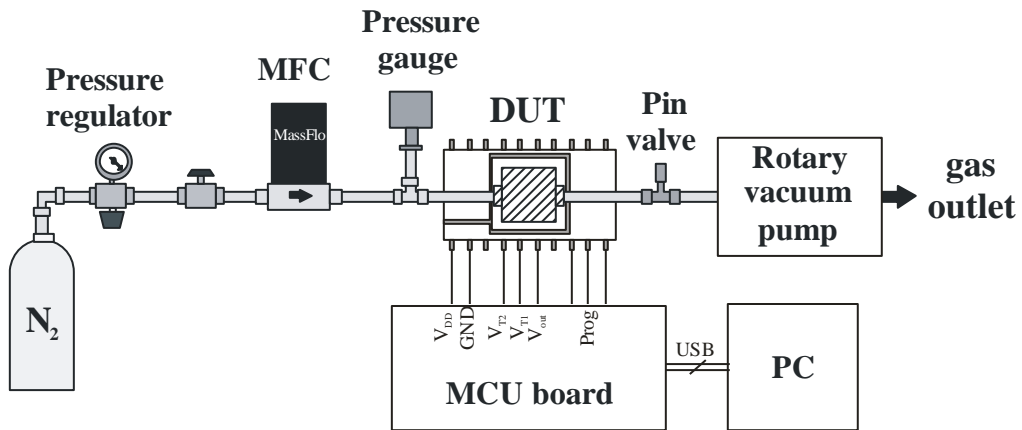


Figure 7

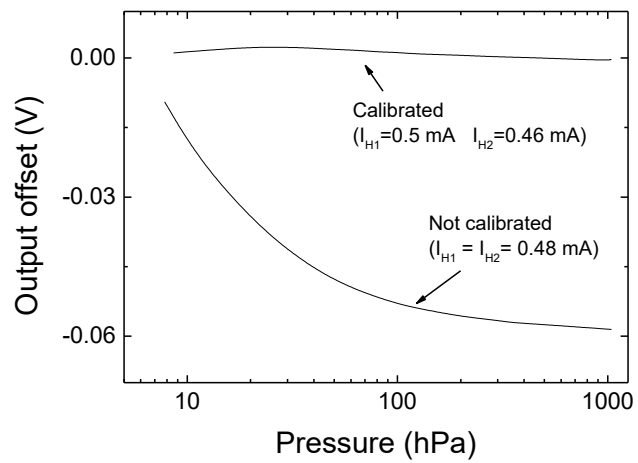


Figure 8

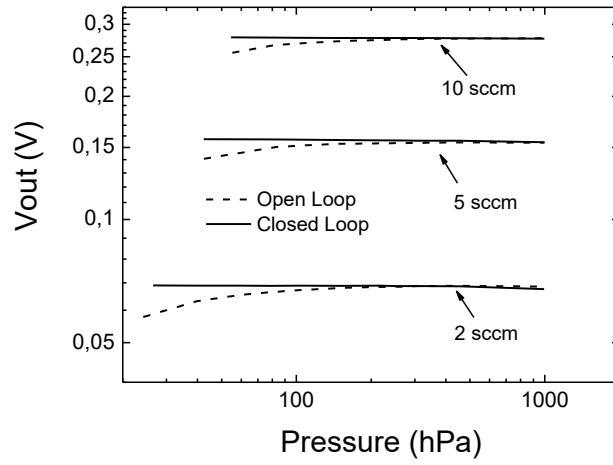


Figure 9

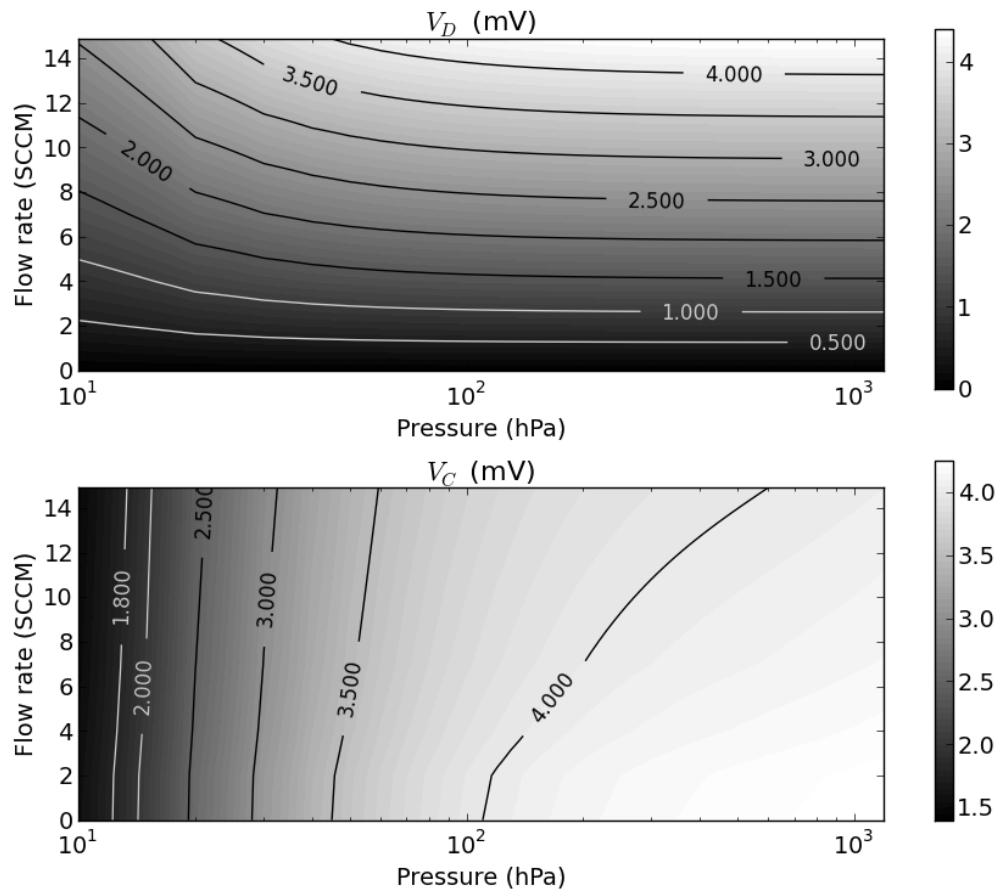


Figure 10

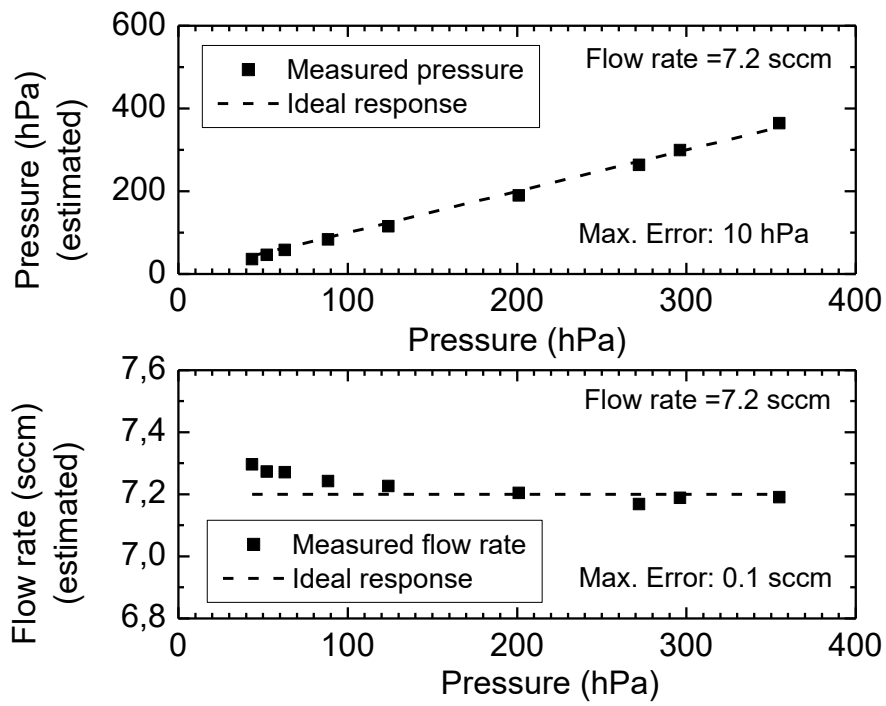


Figure 11